A MAGNETIC STUDY OF LOW MOMENT NICKEL CLUSTERS FORMED FROM THE SOLID-STATE DECOMPOSITION REACTION OF NICKEL BIS-1,5-CYCLOOCTADIENE

ADAM BERLIE, IAN TERRY AND MAREK SZABLEWSKI

Abstract. Variable temperature SQUID magnetometry measurements were made on a sample of commercially available Nickel Bis-1,5-Cyclootcadiene ($Ni(COD)_2$) is reported. The material is shown to be a mixed phase magnetic system where the $Ni(COD)_2$ behaves as a diamagnet containing a paramagnetic component at low temperatures which we believe consists of elemental Ni clusters arising from the decomposition of the material. The magnetic response of the Ni clusters can be described by the combination of two Langevin functions, which indicate cluster magnetic moments of 1.8 μ_B and 15 μ_B suggesting Ni_n clusters with $n = 2 - 3$ and $n = 14 - 19$. However, we demonstrate that these clusters appear to show a spin transition to an $S = 0$ state at low temperatures, which may be a consequence of interactions between the clusters and the surrounding organic medium. Nevertheless, our results suggest that $Ni(COD)_2$ is a novel material for the study of Ni clusters embedded in a diamagnetic background material.

1. Introduction

Nickel Bis-1,5-cyclooctadiene ($Ni(COD)_2$) is a well known source of Ni(0) that has been used and studied for many decades. It was first prepared by Wilke in 1966 and has since found many uses in chemical synthesis due to the ease of oxidation of the nickel[1, 2, 3]. The crystal structure was studied and solved by Direks and Dietrich where the nickel was shown to be in a quasi-tetrahedral environment with carbon-carbon double bonds coordinated to the diamagnetic Ni atom [4]. However, poor orbital overlap results in the COD (1,5-cycloocatdiene) ligands being labile and the structure can fall apart very easily, yielding bulk Ni. Nevertheless, $Ni(COD)_2$ has been used as a starting material for the production of molecular magnetic materials[5]. Since $Ni(COD)_2$ decomposes in air, or on exposure to heat ($T_{Dec} \approx 60°C$)[6], to produce bulk Ni readily, it has become a favourable starting material for making Ni nanoparticles [7, 8, 9, 10], typically by the thermal decomposition of $Ni(COD)_2$ in colloidal systems[11, 12, 13, 14]. Here we report that $Ni(COD)_2$ is also a suitable material for the synthesis and study of magnetic Ni clusters following partial thermal decomposition.

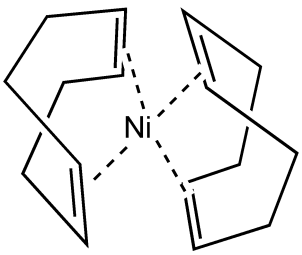

Figure 1. A structural diagram of $Ni(COD)_2$. The structure is quasi-tetrahedral in nature and not square planar.

Atomic clusters are an area of research that has received a large amount of interest, where the physical properties of the clusters behave differently from the bulk [15]. The properties of such sub-nanometer clusters can depend on the number of atoms within the cluster as well as the geometry of the cluster. One example of this is Mn_n clusters where, for $n = 3, 4$, the cluster spins fall into a ferromagnetic groundstate. However for $n = 5$ the cluster can either display a

collinear or non-collinear antiferromagnetic spin arrangement, while, for $n = 6$, the groundstate has non-collinear coupled spins [16]. Experimental work has been conducted on Ni clusters where the magnetic moment was measured as a function of cluster size [17, 18, 19]. It was observed that as the cluster size decreased, generally, the magnetic moment increased. Apsel *et al.*[17] used a Stern-Gerlach deflection technique to determine the cluster size and calculated the magnetic moment using a Langevin function assuming that the clusters were showing a time averaged magnetic moment. They calculated that, for a Ni_5 species, the moment per atom was 1.8 μ_B and this value decreased with increasing cluster size, though the decrease was not monotonic and showed maxima and minima associated with open and closed geometrical shells; the bulk value of 0.61 μ_B was reached when $n = 740$. Billas *et al.* have also conducted some impressive experiments on clusters of Ni, Fe and Co to study the magnetic moment as a function of temperature and cluster size. Their results showed that the magnetic moment increased as the cluster size decreased for Fe, Co and Ni. The temperature dependence of the magnetic moment for the larger clusters of Ni ($n = 140 - 560$) showed a trend similar to that predicted by the Heisenberg Model where the ferromagnetic transition was broadened as a result of small cluster size. For smaller clusters ($n = 40 - 50$) the temperature response of the magnetic moment was different and suggested a constant value up to the Curie temperature where the moment fell rapidly [19].

Theoretical studies have also been carried out on Ni clusters to provide insight into the geometry and moment of individual clusters [20, 21]. Khanna *et al.* modelled the magnetic moment of clusters using a Langevin function where they predicted that the moment rose as $n \rightarrow 2$ however there were variations in the moment due to different geometries causing different surface areas for each value of n. Khanna *et al.* also comment on other predictions of the calculations of magnetic moment carried out by other groups stating that discrepancies may arise if the atomic spacing is considered to be similar to the bulk metal as the clusters moment will be sensitive to the local geometry and exchange distances. Khanna and Reuse used the local density approximation to calculate that for, Ni_3, the moment per atom will equal 0.6 μ_B and for Ni_5, 1.6 μ_B which is close to an experimental result of 1.8 μ_B obtained by Reddy *et al.*[20] and Reuse and Khanna[22] . Khanna *et al.* have also reported that the electronic structure shows band-like behaviour at $n = 14$ suggesting a similarity to bulk behaviour which is radically different to prior experimental data. Very recently Lu *et al.* have calculated geometries and magnetic moments of individual Ni clusters ($n = 2 - 21$) [21]. They observed that when $n = 5 - 10$ stable Ni clusters are formed where the growth is based on a square planar geometry. Also, the groundstate for $n = 2$ is 2 μ_B and as n increases so too does the number of geometries each with their own groundstate magnetic moment; above $n = 10$ the structure becomes more complex.

Within this paper is reported a magnetic study of solid $Ni(COD)_2$ stored under specific conditions usually supposed to maintain material stability. It is demonstrated that the compound always thermally decomposes to components containing differing magnetic phases; one phase is diamagnetic and others are paramagnetic and/or superparamagnetic. We identify the superparamagnetic component as being associated with nickel clusters, the density of which depends upon the storage conditions.

2. Materials and Methods

$Ni(COD)_2$ (purity 98+%) of 2 g quantity was purchased from STREM. The sample was stored under an inert atmosphere in a -20°C freezer (as recommended [23] by the manufacturers) for 2 weeks.

All $Ni(COD)_2$ was handled inside a glovebox under an inert atmosphere (<1 ppm O_2). The material was measured using a specially designed quartz sample holder that could be placed inside a Quantum Design MPMS system [24]. Within the sample holder, the material could be easily and efficiently magnetically characterised while sealed under an inert atmosphere. Field dependent magnetization measurements were made at temperatures between 2 K and 250 K

and at applied magnetic fields of up to 5 T. Transmission electron micrographs and diffraction patterns of $Ni(COD)_2$ were obtained with a JEOL 2100F FEG TEM. Further material for electron microscopy was provided by Sigma Aldrich.

A second batch was also purchased to perform similar experiments and selected results have been included in the manuscript and the complete data can be seen in the supplementary information.

3. Results and Discussion

Field-dependent magnetization data can be seen in figure 1. At 250 K the $Ni(COD)_2$ showed a diamagnetic response that was linear with the applied field, in agreement with previous statements on the magnetic nature of pure $Ni(COD)_2$ [25]. At low fields there is a deviation from the trend line that is due to the competition from the background of the quartz sample holder and signal from the $Ni(COD)_2$ [24]. By fitting a straight line to the data shown in the inset of figure 1 the magnetic susceptibility at 250 K is determined to be χ_D = -4.98(7)$\times 10^{-9}$ m^3kg^{-1}.

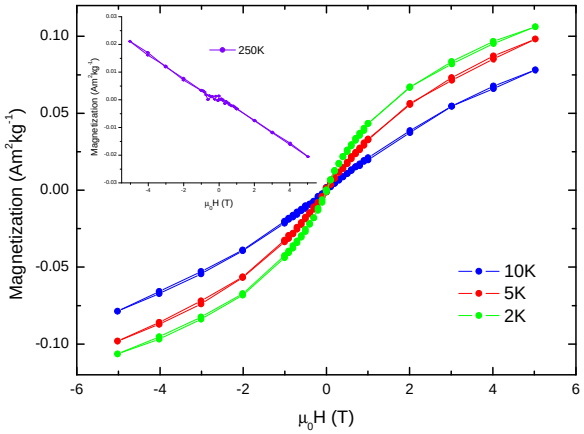

Figure 2. Magnetization vs. applied field, for the 1st batch of $Ni(COD)_2$, taken at 2 K, 5 K and 10 K. Note that no magnetic hysteresis is observed at any temperature. *Inset:* Magnetization vs. applied field at 250 K.

At lower temperatures a large paramagnetic signal dominates the magnetic data. The paramagnetic signal can result from either impurities in the material, defects within the $Ni(COD)_2$ or it may be due to the presence of superparamagnetic nickel nanoparticles or clusters arising from the decomposition of $Ni(COD)_2$. For the case of the 2 K results, the best fit to the data was achieved with a combination of two Langevin functions, which suggests that superparamagnetic nanoparticles are primarily responsible for the paramagnetic response. However, the Langevin function has also been used to describe the low temperature magnetic response of clusters of sub-nanometer scale [20, 17, 26, 27]. The fitting function is given in equation 1, where N is the number of particles per kilogram, μ is the relative magnetic moment, μ_B is the Bohr magneton and k_B is the Boltzmann constant. Fitting parameters are given in table 1 and, using the bulk saturation magnetization value of FCC Ni, it is possible to estimate the mean particle sizes to be 0.7 nm and 0.3 nm corresponding to the larger and smaller of the magnetic moments given in table 1. The values are rather small and suggest such a simple interpretation of the origin of the magnetic moments is not completely correct. In fact the more complicated nature of this magnetic phase is also suggested by attempting to scale the data onto one curve, by plotting magnetization as a function of $\mu_o H/T$, as suggested by equation 1. This can only be achieved if the number density is multiplied by an appropriate scaling factor; this is shown in figure 3 where all the data have been scaled onto the 2 K data set. An interpretation of this result is that there is a temperature dependence of the number density of nanoparticles. For a simple

TABLE 1. Parameters from the fit to the data in figure 3 (see Eqn 1) for both Batches 1 and 2 showing the components α and β. [28] *NB:* Batch 2 were scaled onto the 5 K data set, however this will affect values of N and not the particle sizes.

Batch Number	**Number of Particles per kg** N_j	**Moment** $\langle \mu_{zj} \rangle$ (μ_B)	**Particle Size** (nm)
1(α) 2K	1.6 x 10^{20}	15.1	0.7
1(β) 2K	7.2 x 10^{21}	1.8	0.3
2(α) 5K	1.8 x 10^{20}	38.7	0.9
2(β) 5K	9.2 x 10^{21}	4.3	0.4

superparamagnetic system N should be independent of temperature but it appears as if the number of magnetic moments is decreasing as temperature is lowered, while the mean magnetic moment per particle remains constant.

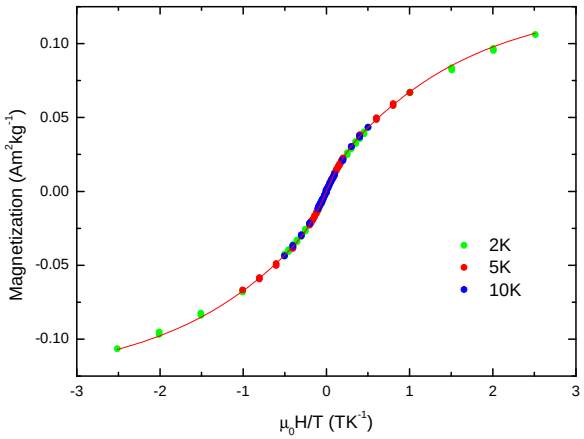

FIGURE 3. Scaled magnetization vs. $\mu_o H/T$ plots for the 1st Batch of $Ni(COD)_2$ at 10 K, 5 K and 2 K. The 5 K and 10 K data have been scaled by dividing the curves by 1.58 and 2.05 respectively where the red curve is a two-term Langevin Function fit to all the data. Note that 50 K data (not shown in the graph) was also taken and can be scaled onto the $\mu_o H/T$ plot using a scaling factor of 3.3.

$$M = (N_\alpha < \mu_\alpha > \mu_B)\left\{\coth(y_\alpha) - \frac{1}{y_\alpha}\right\} + (N_\beta < \mu_\beta > \mu_B)\left\{\coth(y_\beta) - \frac{1}{y_\beta}\right\} \quad (1)$$

$$y = \frac{< \mu > \mu_B \mu_o H}{k_B T} \quad (2)$$

Assuming an FCC (Face Centre Cubic) Ni structure, with the lattice parameter of a = 0.352 nm, the estimated particle sizes listed in table 1 are about 1 - 2 unit cells. However, the particle sizes will only be a rough estimate as within a cluster one would not expect the interatomic distances to be similar to that of the bulk. Nevertheless, the estimate suggests that the thermal decomposition of solid $Ni(COD)_2$ has led to the creation of small clusters containing nickel. For example the decomposition of two unit cells of $Ni(COD)_2$ (the unit cell lattice parameters (a, b & c) are of the order of 7-10 Å), may result in a Ni_2 or Ni_3 clusters

which would be expected to have a magnetic moments of 2 and 2.1 μ_B respectively, according to the LDA calculations of Reuse and Khanna [22]; such values are in reasonable agreement with the 1β moment reported in table 1. However, the fact that two Langevin functions are needed to describe the data of figure 2 may suggest a range of cluster sizes exist within the decomposed $Ni(COD)_2$.

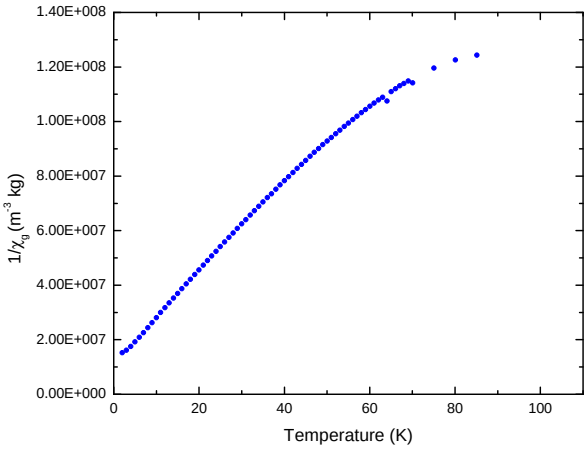

FIGURE 4. Inverse susceptibility vs. temperature of Batch 1. Data were taken with an applied field of 2.5 mT and have been corrected for the diamagnetic susceptibility. Note that the data do not follow a Curie-Weiss law at both high and low temperatures

The scaling of the number density is of interest and indicates that the number of clusters contributing to the total magnetic moment of the sample is decreasing with temperature. One interpretation of this result is that individual clusters are unlikely to adopt an FCC structure and the temperature dependence of N corresponds to spin state transitions within each cluster [29], with thermal excitation from the ground state to various excited states occurring when the temperature is raised above 2 K.

Figure 4 shows that the inverse paramagnetic mass susceptibility is generally a non-linear function of temperature, with the strongest curvature being observed at the highest values of T. However, assuming a Curie-Weiss behaviour at the lowest temperatures the parameters θ = -9 K and $C = 1.2 \times 10^{-6}$ m^3 K kg^{-1} are obtained. Using the total number densities at 2 K (from table 1), the effective moment is estimated to be 6.4 μ_B, in reasonable agreement with the values presented in table 1.

Figure 5 shows the sum total of the saturation magnetization of components α and β from Batch 1 (and Batch 2; see section 2.2) as a function of temperature, deduced from the fits to the results of figure 3 using equation 1. The data show that there is a sharp increase in the saturation magnetization when increasing temperature above 2 K (the 250 K data point is not included in the analysis as it is completely dominated by diamagnetism at this temperature). One interpretation of this result is that the decomposition of $Ni(COD)_2$ at high temperatures has formed small clusters that are not simply HCP (Hexagonal Close Packed) or FCC nanoparticles, and are undergoing a spin transition below 50 K. In fact both the curvature of the $1/\chi$ vs T data and the increase in the saturation magnetization with increasing temperature are both consistent with the thermal excitation of higher spin states within a magnetic cluster [29]. It is known that the effect of adsorbates and ligands on the nickel clusters leads to a singlet ground state for very small clusters and a reduced moment for larger clusters [30, 31, 32, 33]. This is a consequence of an electronic configuration change of the 3d Ni atoms at the surface of the cluster due to the neighbouring adsorbate/ligand [34]. In the case of Ni clusters in $Ni(COD)_2$

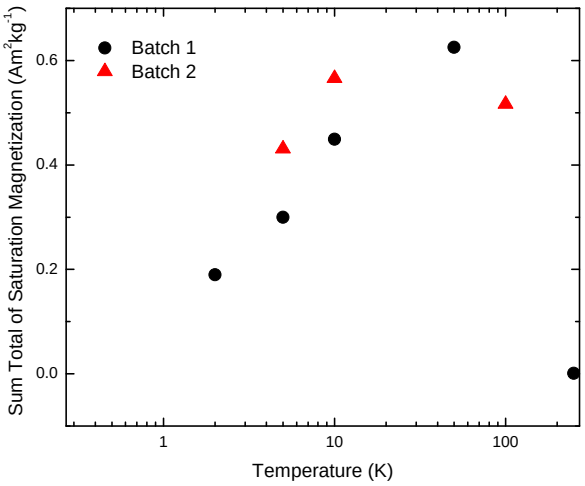

FIGURE 5. Sum total of the saturation magnetization of components α and β of Batches 1 and 2 as a function of temperature. Note that the data point at 250 K is completely dominated by the diamagnetism of the host material.

organic molecules in the decomposed medium, such cyclooctadiene, may act as adsorbates to a cluster causing a ground state with zero, or very low, magnetic moment.

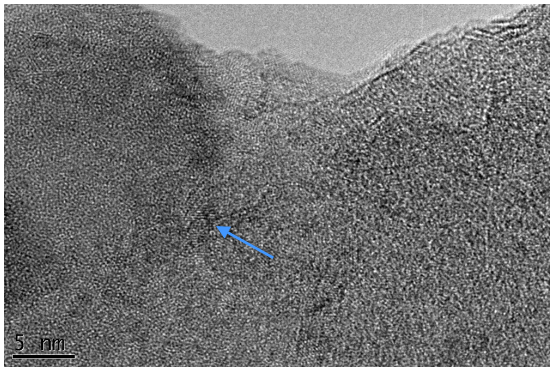

FIGURE 6. High Resolution TEM image of Batch 1. There are no obvious particles that can be seen in the matrix however there may be some crystalline areas approximately 1 nm in dimension (see arrow).

Indirect evidence for the existence of small clusters was obtained from TEM images of batch 1 $Ni(COD)_2$, shown in figure 6. The image does not show any large Ni nanoparticles, but there are some regions that show lattice fringes [35, 36] suggesting very small crystalline areas. These are less then 1 nm in length supporting the particle sizes deduced from the two-term Langevin function fits. It is important to note that it was necessary to record the image in a few seconds because further irradiation with the electron beam resulted in the formation of an assembly of nanoparticles; bright Field and Dark Field TEM images of these e-beam induced particles show that their sizes vary from 2 - 10 nm (see Supplementary Information). Their growth may be due to the electron beam providing thermal energy into the matrix allowing the the Ni clusters to combine and form a larger bulk FCC Ni particle [20]. Electron diffraction patterns (see supplementary information) taken after exposure to the beam indicate crystalline FCC Ni particles do form [37], where the lattice parameters are slightly larger than bulk values, suggesting that there may be a large amount of surface strain on the Ni nanoparticles. These

observations support the conclusions of Rojas *et al.* [38] who reported that electron beam irradiation can promote the growth of FCC nickel particles.

4. Conclusion

The magnetic properties of commercially produced and purchased batches of $Ni(COD)_2$ were measured. The samples showed a mixed magnetic phase system, with evidence characteristic of a diamagnetic response of the host material $Ni(COD)_2$ as well as the presence of nickel clusters which appear to exhibit a temperature induced spin transition at low temperatures. Storing $Ni(COD)_2$ under conditions recommended by the chemical suppliers leads to significant amounts ($\approx$ 2 to 4 % of the sample mass) of smaller moment Ni clusters ($\approx$ 2 to 4 μ_B). These particles/clusters (the β phase) are likely to be a consequence of the thermal decomposition of solid $Ni(COD)_2$. The magnetic moments of the clusters deduced from a combination of Langevin functions are in general agreement with small clusters observed by Apsel *et al.* [17] (Nin $n < 20$) and theoretically investigated by Khanna and Reuse [22] and Lu *et al.* [21].

As an aside, the presence of these low moment clusters does question the use of $Ni(COD)_2$ as a precursor for electronic and magnetic materials. This may be a particular problem when synthesizing molecular magnets as there may be elemental Ni as a contaminant; such a conclusion also made by Miller and Pokhodnya[25] when using $Ni(COD)_2$ with tetracyanoethylene. However, we have shown the promise of $Ni(COD)_2$ as a useful material for study of Ni clusters, though great care must be taken to prevent decomposition of the material to a nanoparticulate or bulk metallic state[24].

5. Acknowledgments

We would like to thank Dr. Budhika Mendis of the Durham G.J. Russell Microscopy Facility and Physics Department for the TEM images. AB wishes to thank the EPSRC for financial support. We would also like to thank Sigma Aldrich for providing further $Ni(COD)_2$ for TEM experiments.

References

[1] G Wilke. *Angew. Chem. Int. Ed* **72** 581 (1960).
[2] B. Bogdanov, M. Kroner and G. Wilke. *Liebigs Ann. Chem.* **Nov** 699 (1966).
[3] W. Keim. *Angew. Chem. Int. Ed.* **29** 235 (1990).
[4] H. Dierks and H. Dietrich. *Z. Kristallogr.* **122** 1 (1965)
[5] R Jain, K Kabir, J.B Gilroy, K.A.R Mitchell, K.C Wong and R.G Hicks. *Nature* **445** 291 (2007)
[6] R. A. Schunn, S. D. Ittel and M. A. Cushing *Inorganic Syntheses* **28** 94 (1990)
[7] T Ould-Ely, C Amiens and B Chaudret. *Chem. Mater.* **11** 526 (1999)
[8] N Cordente, C Amiens, B Chaudret, M Respaud, F Senocq and M. J Casanove. *J. App. Phys.* **94** 6358 (2003)
[9] Y Koltypin, A Fernadez, T Critina Rojas, J Campora, P Palmer, R Prozorov and A Gedanken. *Chem. Mater.* **11** 1331 (1999)
[10] P. B Oliete, T Critina Rojas, A Fernadez, T Critina Rojas, A Gedanken, Y Koltypin and F Palacio. *Acta Materialia* **11** 2165 (2004)
[11] D. de Caro and J.S. Bradley. *Langmuir***13** 3067 (1997)
[12] J.S. Bradley, B. Tesche, W. Busser, M. Maase, and M.T. Reetz. *J. Am. Chem. Soc.* **122** 4631 (2000)
[13] G. Cheng, V.F. Puntes, and T. Guo. *J. Colloid Interface Sci.* **293** 430 (2006)
[14] E. Ramirez-Meneses, I. Betancourt, F. Morales, V. Montiel-Palma, C.C. Villanueva-Alvarado, and M.E. Hernandez-Rojas. *J. Nanopart. Res.* **13** 365 (2011)
[15] A. W Castleman, Jr. and S. N Khanna. *J. Phys. Chem.* **113** 2664 (2008)
[16] T Morisato, S. N Khanna and Y Kawazoe. *Phys. Rev. B.* **72** 014435 (2005)
[17] S. E Apsel, J. W Emmert, J Deng and L. A Bloomfield. *Phys. Rev. Letts.* **76** 1441 (1996)
[18] I. M. L Billas, A Châtelain and W. A de Heer. *J. Magn. Magn. Mater.* **168** 64 (1997)
[19] I. M. L Billas, A Châtelain and W. A de Heer. *Science* **265** 1682 (1994)
[20] B. V Reddy, S. K Nayak, S.N Khanna, B.K Rao and P Jena. *J. Phys. Chem. A.* **102** 1748 (1998)
[21] Q. L Lu, Q. Q Luo, L. L Chen and J. G Wan. *Eur. Phys. D.* **61** 389 (2011)
[22] F. A Reuse and S. N Khanna. *Chem. Phys. Letts.* **234** 77 (1995)
[23] Sigma-Aldrich. *Bis(1,5-cyclooctadiene)Nickel MDMS.* www.sigmaaldrich.com, 25 Jan 2010.
[24] A Berlie, I Terry and M Szablewski. *Meas. Sci. Technol.* **22** 017002 (2011).
[25] J. S Miller and K. I Pokhodnya. *J. Mater. Chem.* **17** 3585 (2007)
[26] Xi Chen, S Bedanta, O Petracic, W Kleemann, S Sahoo, S Cardoso and P. P Freitas *Phys. Rev. B* **72** 214436 (2005)
[27] O Okada. *J. Phys. Soc. Japan* **48** 391 (1980).
[28] For the first Batch the average error in the fit is 9 % which is substantial however this error is vastly increased when translated to particle size where it becomes 37 %. The error in the particle size is not reflective of the fit to the data by Equation 1 as the overall fit has a R^2 value of 0.999 showing a good fit. For Batch 2 the errors in the fit to the data average out at 6 % which translates to a 35 % error in the particle size where the fit has an R^2 value of 0.999.
[29] J. S Smart Evaluation of Exchange Interactions from Experimental Data *Magnetism III* ed. GT Rado and J Suhl Academic Press, New York and London, 1963 63-114.
[30] D. A. van Leeuwen, J.M. van Ruitenbeek, L.J. de Jongh, A. Ceriotti, G. Pacchioni, O.D. Häberlen and N. Rösch *Phys. Rev. Lett.* **73** 1432 (1994)
[31] M.B. Knickelbein. *J. Chem. Phys.* **116** 9703 (2002)
[32] F.A Reuse, S. N. Khanna, B.V. Reddy and J. Buttet *Chem. Phys. Letts.* **267** 258 (1997)
[33] G. Pacchioni and N. Rösch. *Acc. Chem. Res.* **28** 390 (1990)
[34] N. Rösch, L. Ackermann and G. Pacchioni *J. Am. Chem. Soc.* **114** 3549 (1995)
[35] D. B Williams and C Barry Carter. Transmission Electron Microscopy Imaging III 1996 New York: Kluwer Academic/ Plenum Publishers 441-444
[36] P Fraundorf, W Qin, P Moeck and E Mandell. *J. App. Phys* **98** 114308 (2005)
[37] When looking at the ratio of diffraction planes to confirm a FCC cubic phase we should get from the (111):(200) = 1.33 and from (220):(111) = 2 and from (111):(113) = 2.75. We observe 1.38 and 1.93 before imaging and 1.37, 2.02 and 2.97 respectively after imaging.
[38] T. C. Rojas, M. J. Sayagués, A. Caballero, Y. Koltypin, A. Gedanken, L. Ponsonnet, B. Vacher, J. M. Martin and A Fernández. *J. Chem. Mater.* **10** 715 (2000)